crystallization communications

Crystallization and preliminary X-ray diffraction studies of the transcriptional repressor PaaX, the main regulator of the phenylacetic acid degradation pathway in *Escherichia coli* W

Alzoray Rojas-Altuve,[a] César Carrasco-López,[a] Víctor M. Hernández-Rocamora,[b]‡ Jesús M. Sanz[b] and Juan A. Hermoso[a]*

[a]Grupo de Cristalografía Macromolecular y Biología Estructural, Instituto de Química-Física Rocasolano, CSIC, Serrano 119, 28006 Madrid, Spain, and [b]Instituto de Biología Molecular y Celular, Universidad Miguel Hernández, Avenida Universidad s/n, 03202 Elche, Spain

‡ Present address: Centro de Investigaciones Biológicas, Consejo Superior de Investigaciones Científicas, Ramiro de Maeztu 9, 28040 Madrid, Spain.

Correspondence e-mail: xjuan@iqfr.csic.es

PaaX is the main regulator of the phenylacetic acid aerobic degradation pathway in bacteria and acts as a transcriptional repressor in the absence of its inducer phenylacetyl-coenzyme A. The natural presence and the recent accumulation of a variety of highly toxic aromatic compounds owing to human pollution has created considerable interest in the study of degradation pathways in bacteria, the most important microorganisms capable of recycling these compounds, in order to design and apply novel bioremediation strategies. PaaX from *Escherichia coli* W was cloned, overexpressed, purified and crystallized using the sitting-drop vapour-diffusion method at 291 K. Crystals grew from a mixture of 0.9 M Li$_2$SO$_4$ and 0.5 M sodium citrate pH 5.8. These crystals, which belonged to the monoclinic space group $C2$ with unit-cell parameters a = 167.88, b = 106.23, c = 85.87 Å, β = 108.33°, allowed the collection of an X-ray data set to 2.3 Å resolution.

1. Introduction

After carbohydrates, aromatic compounds are the most abundant class of organic compounds used by nature (Harwood & Parales, 1996) and their concentrations have recently increased in many ecosystems as a consequence of human pollution (OECD, 1994). Microorganisms, mostly bacteria, recycle both natural and man-made aromatic compounds. In this sense, the degradation pathways used by these microorganisms are highly relevant in the field of bioremediation, which uses microorganisms or their enzymes to eliminate pollutants from contaminated environments (Ramos *et al.*, 1994; Harwood & Parales, 1996; Pieper & Reineke, 2000).

In bacteria, aerobic degradation of phenylacetic acid (PAA) begins with the esterification of PAA with coenzyme A (CoA) by phenylacetyl-CoA (PA-CoA) ligase, which is common to anaerobic degradation pathways (Luengo *et al.*, 2001), in contrast to the degradation of hydroxylated PAA derivatives. In *Escherichia coli* W, *paa* gene clusters code for enzymes that aerobically degrade PAA (Ferrández *et al.*, 1998). Homologues of *paa* genes have been found in different microorganisms, all of which have similar regulation mechanisms (García *et al.*, 2000; Rost *et al.*, 2002; Navarro-Llorens *et al.*, 2005; del Peso-Santos *et al.*, 2006; Di Gennaro *et al.*, 2007).

The transcriptional repressor PaaX (315 amino acids, 35 295 Da; Ferrández *et al.*, 1998) encoded in one of the *paa* clusters represses the expression of the PAA aerobic degradation pathway enzymes, binding to the operator sequences in the *paa* gene clusters in the absence of PA-CoA and therefore blocking transcription by RNA polymerase. When the PA-CoA concentration increases the repressor is released from the DNA, allowing transcription to proceed. Additionally, PaaX regulates the expression of degradation pathways that produce PAA as their final product, such as penicillin G acylase (PGA), which hydrolyses numerous esters and amines of phenylacetic acid (Galán *et al.*, 2004; Kim *et al.*, 2004), and the styrene-degradation pathway in *Pseudomonas* sp. strain Y2 (del Peso-Santos *et al.*, 2006). Hence, PaaX is currently considered to be a central regulator in the aerobic degradation of aromatic compounds derived from PAA in several microorganisms (Luengo *et al.*, 2001).

Table 1
Data-collection statistics for PaaX crystals.

Values in parentheses are for the highest resolution shell.

Crystal data	
Space group	$C2$
Unit-cell parameters	
a (Å)	167.88
b (Å)	106.23
c (Å)	85.87
β (°)	108.33
Data processing	
Temperature (K)	100
Wavelength (Å)	0.9334
Resolution (Å)	44.2–2.3 (2.4–2.3)
Unique data	63547
Multiplicity	3.7 (3.7)
Data completeness (%)	99.9 (99.9)
Average $I/\sigma(I)$	20.9 (2.8)
Molecules in asymmetric unit	4
Matthews coefficient (Å^3 Da^{-1})	2.89
Solvent content (%)	61
R_{merge}†	0.05 (0.49)

† $R_{merge} = \sum_{hkl} \sum_i |I_i(hkl) - \langle I(hkl) \rangle| / \sum_{hkl} \sum_i I_i(hkl)$, where $I_i(hkl)$ is the ith measurement of reflection hkl and $\langle I(hkl) \rangle$ is the weighted mean of all measurements.

PaaX is classified in the Pfam database as a member of the PaaX-like protein family (http://pfam.sanger.ac.uk/family/PF07848), which encompasses transcriptional regulators of the PAA-degradation pathway in several proteobacteria. The N-terminal region of PaaX-like proteins has sequence homology to the winged helix–turn–helix (wHTH) motif of the GntR family of transcriptional regulators, while the C-terminal region bears no homology to other protein families (Ferrández *et al.*, 2000; Tropel & van der Meer, 2004). Therefore, it has been speculated that PaaX comprises two domains, with the N-terminal domain being in charge of binding DNA and repressing transcription, while the C-terminal domain binds the PA-CoA activator and regulates the activity of the N-terminal domain (Ferrández *et al.*, 2000). Interestingly, the proposed palindromic consensus DNA-binding sequence of PaaX has a separation of 25 bp between the two halves of the palindrome (Kim *et al.*, 2004), which is unprecedented in transcriptional regulators of the GntR family.

Although the function of PaaX has been thoroughly studied, structural studies are absent from the literature. Only two structures from the PaaX-like protein family have been deposited in the PDB (PDB entries 3l09 from *Jannaschia* sp. and 3kfw from *Mycobacterium tuberculosis*; Joint Center for Structural Genomics, unpublished work; U. A. Ramagopal, R. Toro, S. K. Burley & S. C. Almo, unpublished work) and preliminary crystallization and X-ray analyses have been reported for a PaaX-like protein (Cao *et al.*, 2009). However, no further analysis of these structures has been published.

In this work, we report the crystallization and preliminary X-ray diffraction studies of a cysteine-lacking variant of PaaX from *E. coli* W.

2. Experimental

2.1. *E. coli* PaaX expression and purification

A hexahistidine-tagged cysteine-lacking variant of PaaX, HisPaaX C4, was purified from pX2BSc0 plasmid in *E. coli* MV1184 cells (Sambrook & Russell, 2001). This mutant conserves its DNA-binding and transcription-activation functionality, as well as the overall structure and stability of the wild-type form (Hernández-Rocamora *et al.*, unpublished results). A fresh transformant colony was grown overnight at 310 K. The culture was diluted 100-fold in 1 l LB medium and grown at 303 K until the optical density at 600 nm

reached 0.5–0.6. Overexpression was induced by the addition of isopropyl β-D-1-thiogalactopyranoside (IPTG) to a concentration of 1 m*M* followed by further incubation at 303 K for 16 h.

Cultures were harvested by centrifugation at 3000*g* for 15 min at 277 K. The cells were resuspended in 40 ml Im20 buffer (50 m*M* sodium phosphate pH 8 with 300 m*M* NaCl and 20 m*M* imidazole) and sonicated on ice in a Branson 250 sonicator. The soluble protein fraction was separated by centrifugation at 100 000*g* for 1 h at 277 K.

Supernatants were mixed in batches with 5 ml chelating Sepharose (Chelating Sepharose Fast Flow, GE Healthcare) loaded with Ni and gently stirred for 1 h at room temperature (RT). The Sepharose with the absorbed protein was packed into a column and washed consecutively with two column volumes of Im20 buffer and two column volumes of Im100 buffer (as Im20 but with 40 m*M* imidazole). PaaX was eluted with Im400 buffer (20 m*M* Tris–HCl pH 8 with 500 m*M* NaCl and 400 m*M* imidazole). The fractions containing the highest concentrations of PaaX (measured using UV absorbance; the purity was checked by SDS–PAGE) were pooled. Samples were frozen quickly in a dry-ice/ethanol bath and stored at 193 K.

2.2. Crystallization

Initial crystallization assays based on the commercial screens JCSG+ Suite and PACT Suite from Qiagen and Crystal Screen and Crystal Screen 2 from Hampton Research were carried out by high-throughput techniques using a NanoDrop ExtY robot (Innovadyne Technologies Inc.). All crystallization trials were performed by the sitting-drop vapour-diffusion method at 291 K in Innovaplate SD-2 microplates (Innovadyne Technologies Inc.), mixing equal amounts (250 nl) of PaaX solution at 9.7 mg ml^{-1} [20 m*M* Tris pH 8, 500 m*M* NaCl, 400 m*M* imidazole and 20%(*v/v*) glycerol] and precipitant solution. The drops (500 nl) were equilibrated against 65 µl precipitant solution. Optimized crystals were obtained by scaling up the drop volume using the sitting-drop method: 1 µl PaaX solution was mixed with 1 µl precipitant solution and equilibrated against 500 µl precipitant solution.

2.3. Diffraction data collection and processing

Crystals were soaked for 5 s in a cryoprotectant solution [20%(*v/v*) glycerol in the crystallization mother liquor] prior to flash-cooling at 100 K by direct transfer into liquid nitrogen using a cryogenic system. X-ray data sets were collected using synchrotron radiation at the ESRF, Grenoble, France. A data set was collected from a PaaX
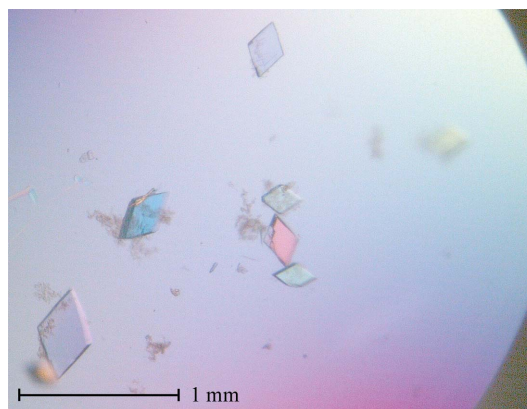
Figure 1
PaaX crystals obtained with 0.9 *M* lithium sulfate and 0.5 *M* sodium citrate pH 5.8 under polarized light. The approximate dimensions of the crystals are 0.15 × 0.4 × 0.4 mm.
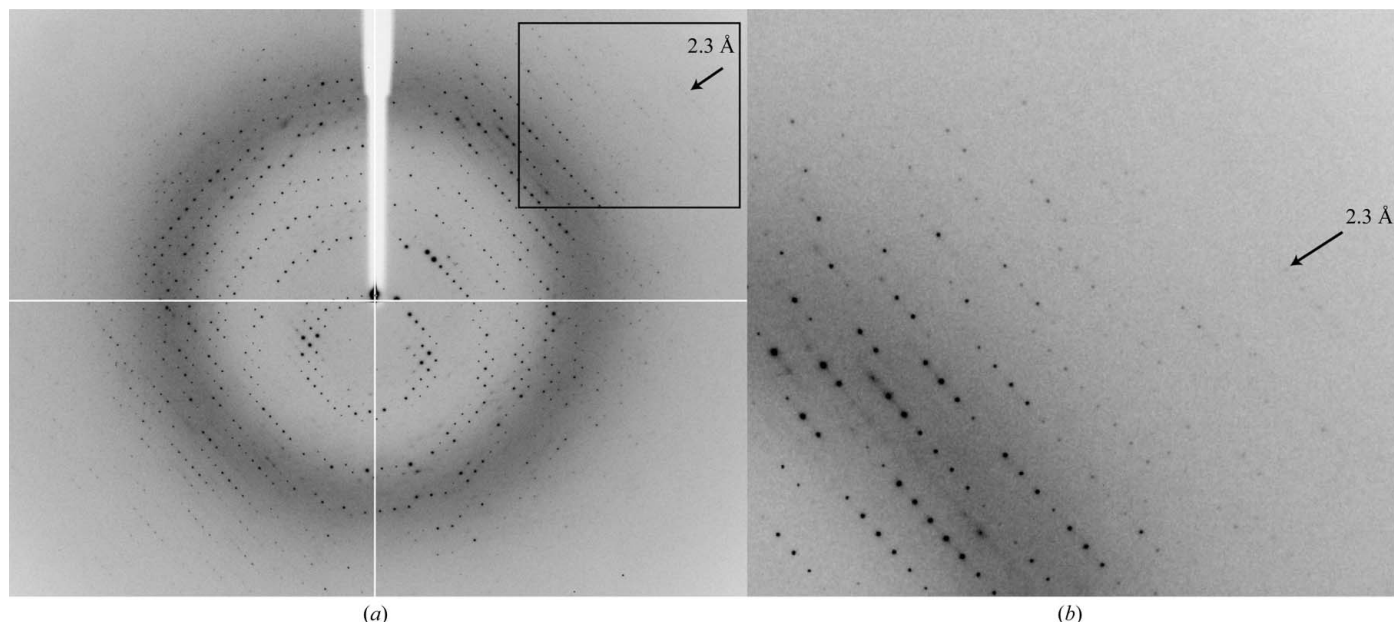
Figure 2
(*a*) X-ray diffraction pattern of PaaX crystals; (*b*) an enlargement showing high-resolution spots.

crystal to 2.3 Å resolution on beamline ID14-1 ($\lambda = 0.93340$ Å) using an ADSC Quantum Q210 detector (oscillation range 1°, crystal-to-detector distance 191.64 mm). The diffraction data were processed using the *XDS* program (Kabsch, 2010) and scaled using *SCALA* (Evans, 1993) from the *CCP*4 program suite (Winn *et al.*, 2011); processing data are summarized in Table 1.

3. Results

A fully functional PaaX variant containing an N-terminal hexahistidine tag and with all four cysteine residues present in the wild-type protein substituted by alanines was constructed (Hernández-Rocamora *et al.*, unpublished results) in order to increase the stability during purification and to avoid aggregation at the concentrations required for crystallization purposes.

PaaX microcrystals grew from condition No. 15 of Crystal Screen 2 (1.0 *M* lithium sulfate, 0.5 *M* ammonium sulfate and 0.5 *M* sodium citrate pH 5.6). Good-quality crystals of PaaX were obtained from optimized conditions (0.9 *M* lithium sulfate and 0.5 *M* sodium citrate pH 5.8; Fig. 1). An X-ray data set was collected to 2.3 Å resolution. The images displayed good-quality diffraction patterns (Fig. 2). Preliminary X-ray data processing showed good statistics (Table 1). The crystal belonged to the monoclinic space group *C*2, with unit-cell parameters $a = 167.88$, $b = 106.23$, $c = 85.87$ Å, $\beta = 108.33°$. Specific volume calculations based on the molecular weight of PaaX (32 kDa) and the unit-cell parameters (volume = 1 458 706.8 Å^3) indicated the possible presence of four monomer molecules in the asymmetric unit with 61% solvent content ($V_M = 2.89$ Å^3 Da^{-1}; Matthews, 1968).

Structural determination of PaaX by the molecular-replacement method using the structural model from *Jannaschia* sp. (PDB entry 3l09; Joint Center for Structural Genomics, unpublished work), which shows 30% sequence homology, is currently in progress.

References

Cao, Y., Lou, Z., Sun, Y., Xue, F., Feng, C., Gong, X., Yang, D., Bartlam, M., Meng, Z. & Zhang, K. (2009). *Acta Cryst.* F**65**, 776–778.
Di Gennaro, P., Ferrara, S., Ronco, I., Galli, E., Sello, G., Papacchini, M. & Bestetti, G. (2007). *Arch. Microbiol.* **188**, 117–125.
Evans, P. R. (1993). *Proceedings of the CCP4 Study Weekend. Data Collection and Processing*, edited by L. Sawyer, N. Isaacs & S. Bailey, pp. 114–122. Warrington: Daresbury Laboratory.
Ferrández, A., García, J. L. & Díaz, E. (2000). *J. Biol. Chem.* **275**, 12214–12222.
Ferrández, A., Miñambres, B., García, B., Olivera, E. R., Luengo, J. M., García, J. L. & Díaz, E. (1998). *J. Biol. Chem.* **273**, 25974–25986.
Galán, B., García, J. L. & Prieto, M. A. (2004). *J. Bacteriol.* **186**, 2215–2220.
García, B., Olivera, E. R., Miñambres, B., Carnicero, D., Muñiz, C., Naharro, G. & Luengo, J. M. (2000). *Appl. Environ. Microbiol.* **66**, 4575–4578.
Harwood, C. S. & Parales, R. E. (1996). *Annu. Rev. Microbiol.* **50**, 553–590.
Kabsch, W. (2010). *Acta Cryst.* D**66**, 125–132.
Kim, H. S., Kang, T. S., Hyun, J. S. & Kang, H. S. (2004). *J. Biol. Chem.* **279**, 33253–33262.
Luengo, J. M., García, J. L. & Olivera, E. R. (2001). *Mol. Microbiol.* **39**, 1434–1442.
Matthews, B. W. (1968). *J. Mol. Biol.* **33**, 491–497.
Navarro-Llorens, J. M., Patrauchan, M. A., Stewart, G. R., Davies, J. E., Eltis, L. D. & Mohn, W. W. (2005). *J. Bacteriol.* **187**, 4497–4504.
OECD (1994). *Biotechnology for a Clean Environment: Prevention, Detection and Remediation*. Paris: OECD Press.
Peso-Santos, T. del, Bartolomé-Martín, D., Fernández, C., Alonso, S., García, J. L., Díaz, E., Shingler, V. & Perera, J. (2006). *J. Bacteriol.* **188**, 4812–4821.
Pieper, D. H. & Reineke, W. (2000). *Curr. Opin. Biotechnol.* **11**, 262–270.
Ramos, J. L., Díaz, E., Dowling, D., de Lorenzo, V., Molin, S., O'Hara, F., Ramos, C. & Timmis, K. N. (1994). *Biotechnology*, **12**, 1349–1356.
Rost, R., Haas, S., Hammer, E., Herrmann, H. & Burchhardt, G. (2002). *Mol. Genet. Genomics*, **267**, 656–663.
Sambrook, J. & Russell, D. W. (2001). *Molecular Cloning: a Laboratory Manual*, 3rd ed. Cold Spring Harbor Laboratory Press.
Tropel, D. & van der Meer, J. R. (2004). *Microbiol. Mol. Biol. Rev.* **68**, 474–500.
Winn, M. D. *et al.* (2011). *Acta Cryst.* D**67**, 235–242.